

Supplemental Information

**Inc-Rps4l-encoded peptide RPS4XL regulates
RPS6 phosphorylation and inhibits the
proliferation of PSMCs caused by hypoxia**

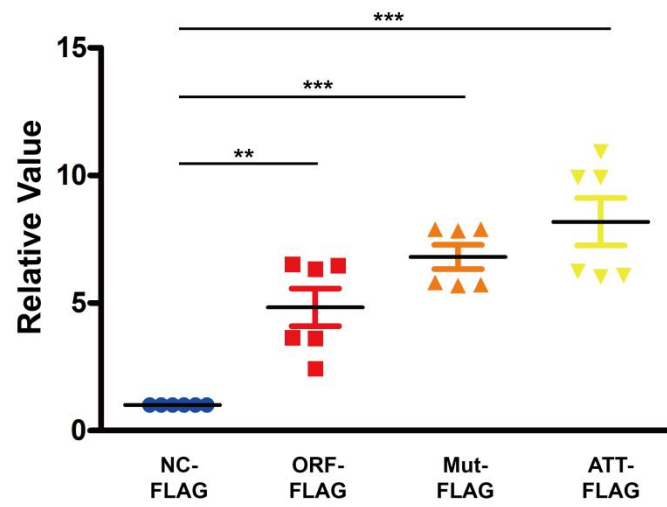
Yiying Li, Juntong Zhang, Hanliang Sun, Yujie Chen, Wendi Li, Xiufeng Yu, Xijuan Zhao, Lixin Zhang, Jianfeng Yang, Wei Xin, Yuan Jiang, Guilin Wang, Wenbin Shi, and Daling Zhu

Supplemental material
Figure S1



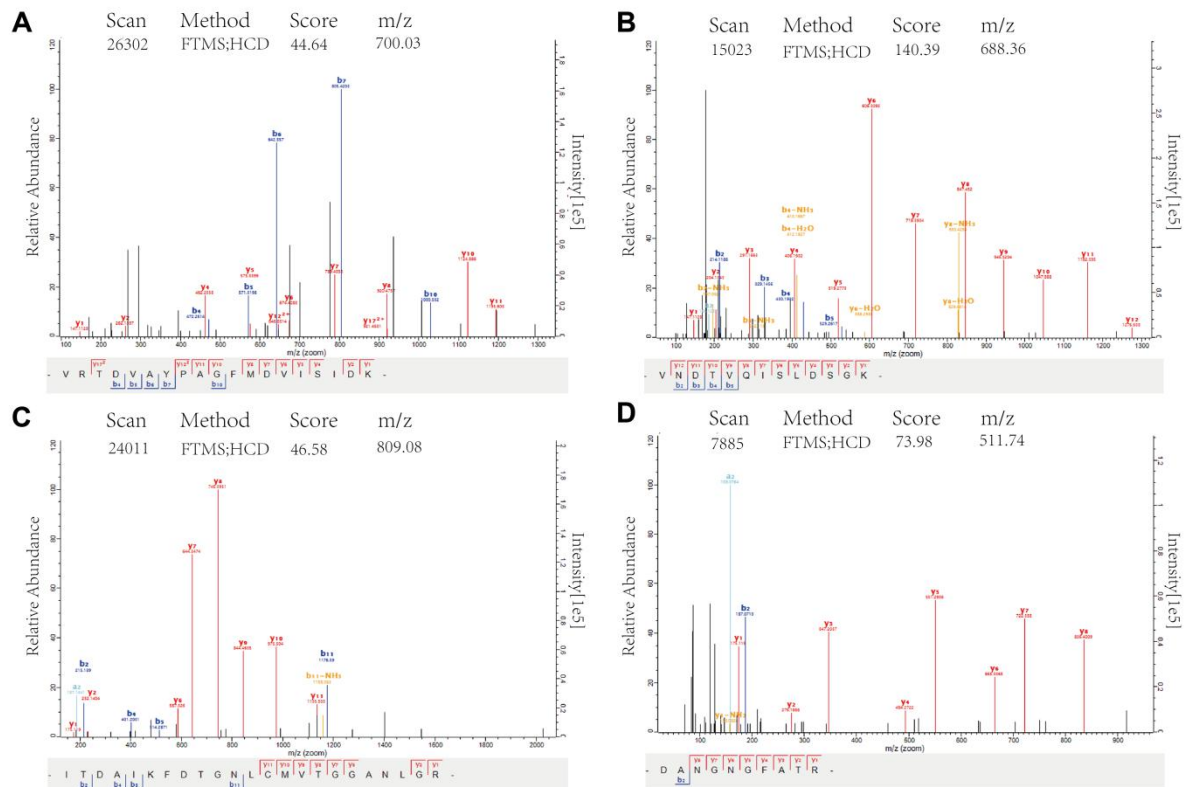
Supplemental figure 1. Rps4l's open reading frame and coding sequence were detected by ExPASy.

Figure S2



Supplemental figure 2. Overexpression efficiency of the plasmid were used. All values are represented as the mean \pm SEM (**p < 0.01, and ***p < 0.001; n \geq 3).

Figure S3



Supplemental figure 3. Mass spectrum of the RPS4XL. (A) Mass spectrum of RPS4XL amino acids 76-94. (B) Mass spectrum of RPS4XL amino acids 156-168. (C) Mass spectrum of RPS4XL amino acids 169-191. (D) Mass spectrum of RPS4XL amino acids 212-221.

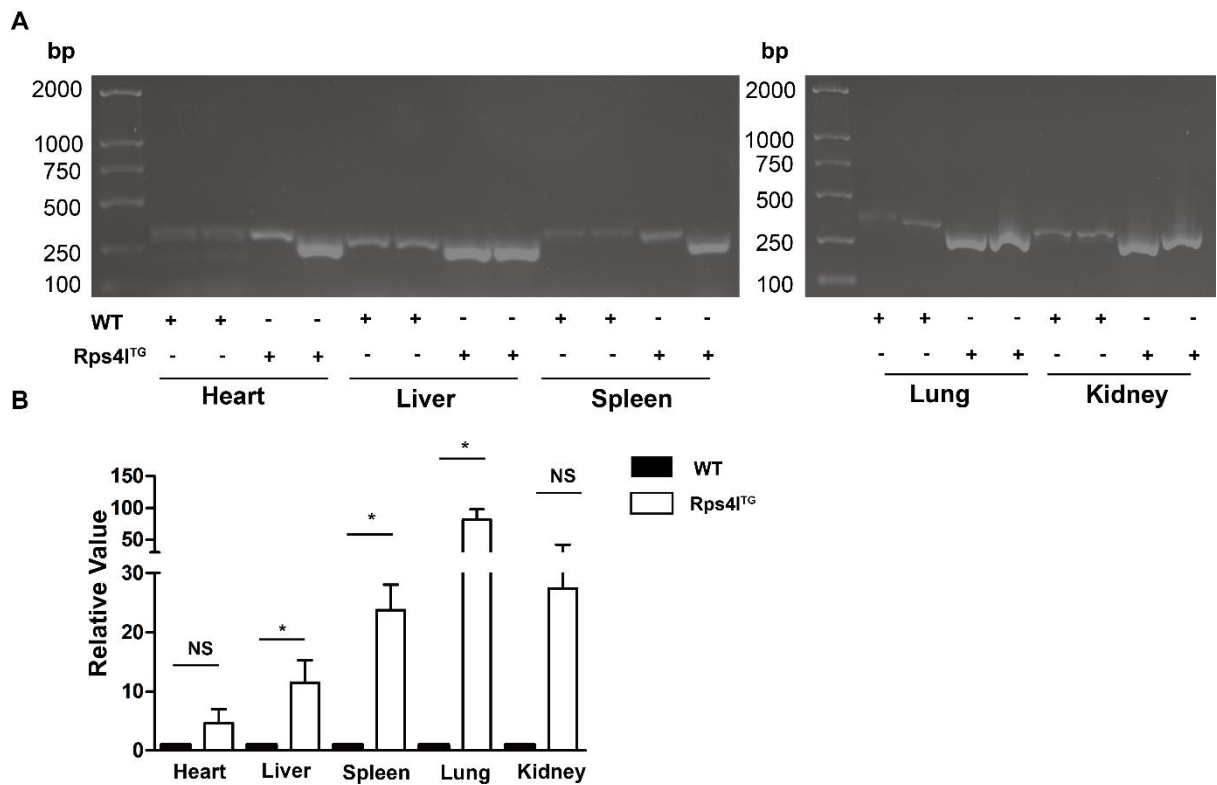
Figure S4



Supplemental figure 4. Detection of the specificity of anti-RPS4XL antibody. (A)

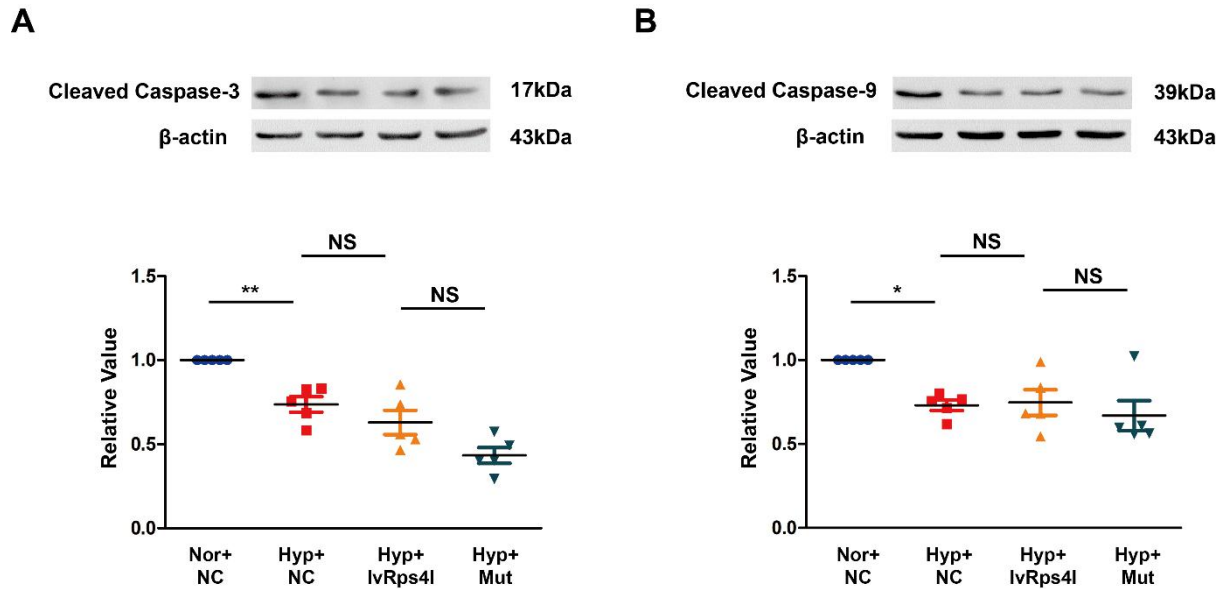
Western blot analysis of expression of RPS4XL detected by the antibody in PASCs treated with lvRps4l or NC. (B) Western blot analysis of expression of RPS4XL detected by the antibody in PASCs treated with si-Rps4l or si-NC.

Figure S5



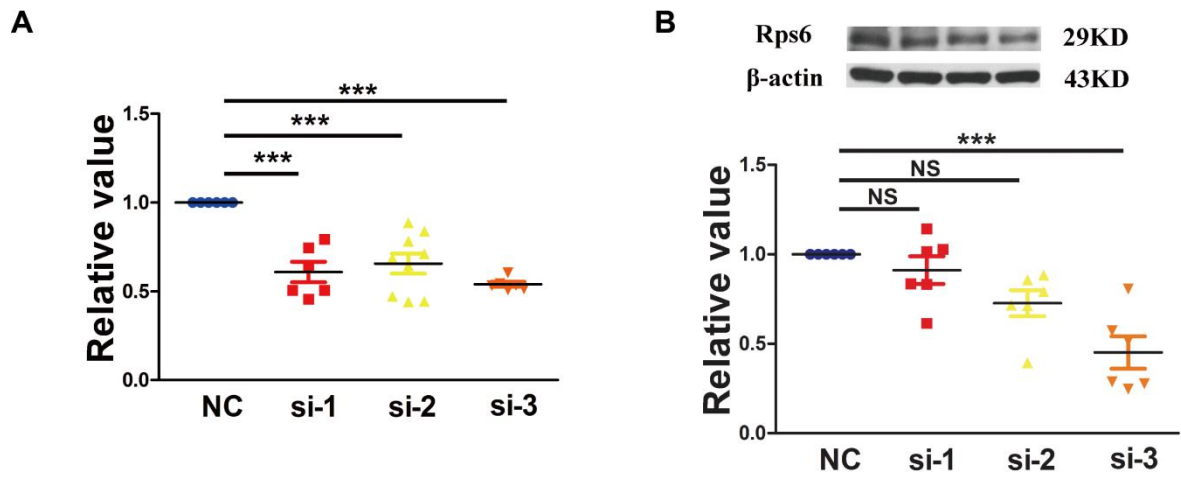
Supplemental figure 5. Expression of Rps4l in different organs of overexpression transgenic mice. (A) Agarose gel electrophoresis of the expression of Rps4l in the heart, liver, spleen, lung and kidney of WT and Rps4lTg mice. (B) qPCR analysis of the overexpression efficiency of Rps4l in the heart, liver, spleen, lung and kidney of Rps4l mice. All values are represented as the mean \pm SEM (* p <0.05 and NS, no significance; $n \geq 3$).

Figure S6



Supplemental figure 6. RPS4XL does not regulate hypoxia-induced inhibition of apoptosis in PSMCs. (A) WB analysis of cleaved caspase-3 in hypoxic and control PSMCs transfected with lvRps4l, ORFmut, or NC. (B) WB analysis of cleaved caspase-9 in hypoxic and control PSMCs transfected with lvRps4l, ORFmut, or NC. All values are represented as the mean \pm SEM (* $p < 0.05$, ** $p < 0.01$ and NS, no significance; $n \geq 3$).

Figure S7



Supplemental figure 7. Interference efficiency of three RNAi of Rps6 in PSMCs.

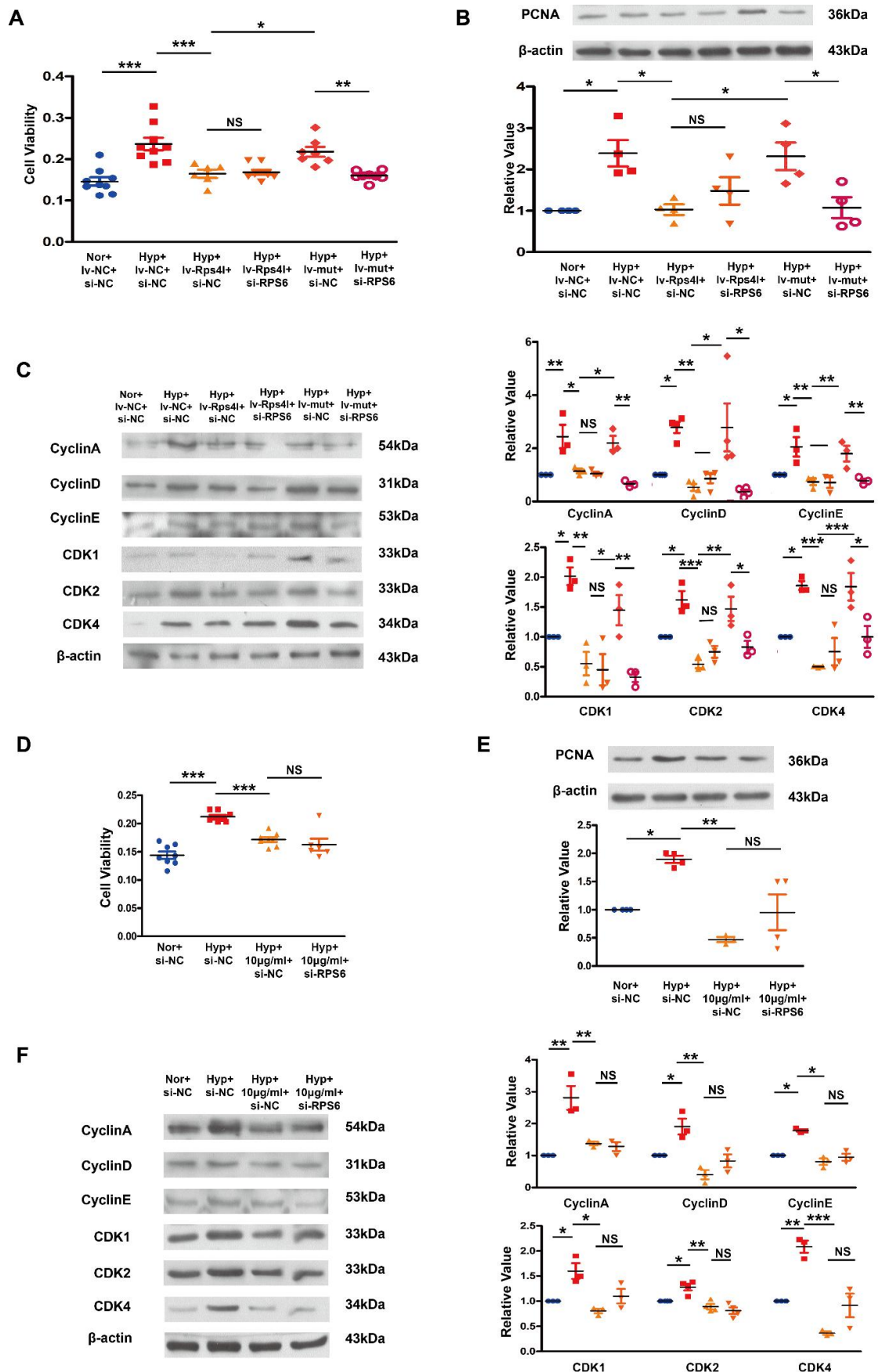
The si-3 was used in this study. (A) Interference efficiency of RPS6 in mRNA level.

(B) Interference efficiency of RPS6 in protein level. Si-3 was used for the study. All

values are represented as the mean \pm SEM (***) $p < 0.001$ and NS, no significance; n

≥ 3).

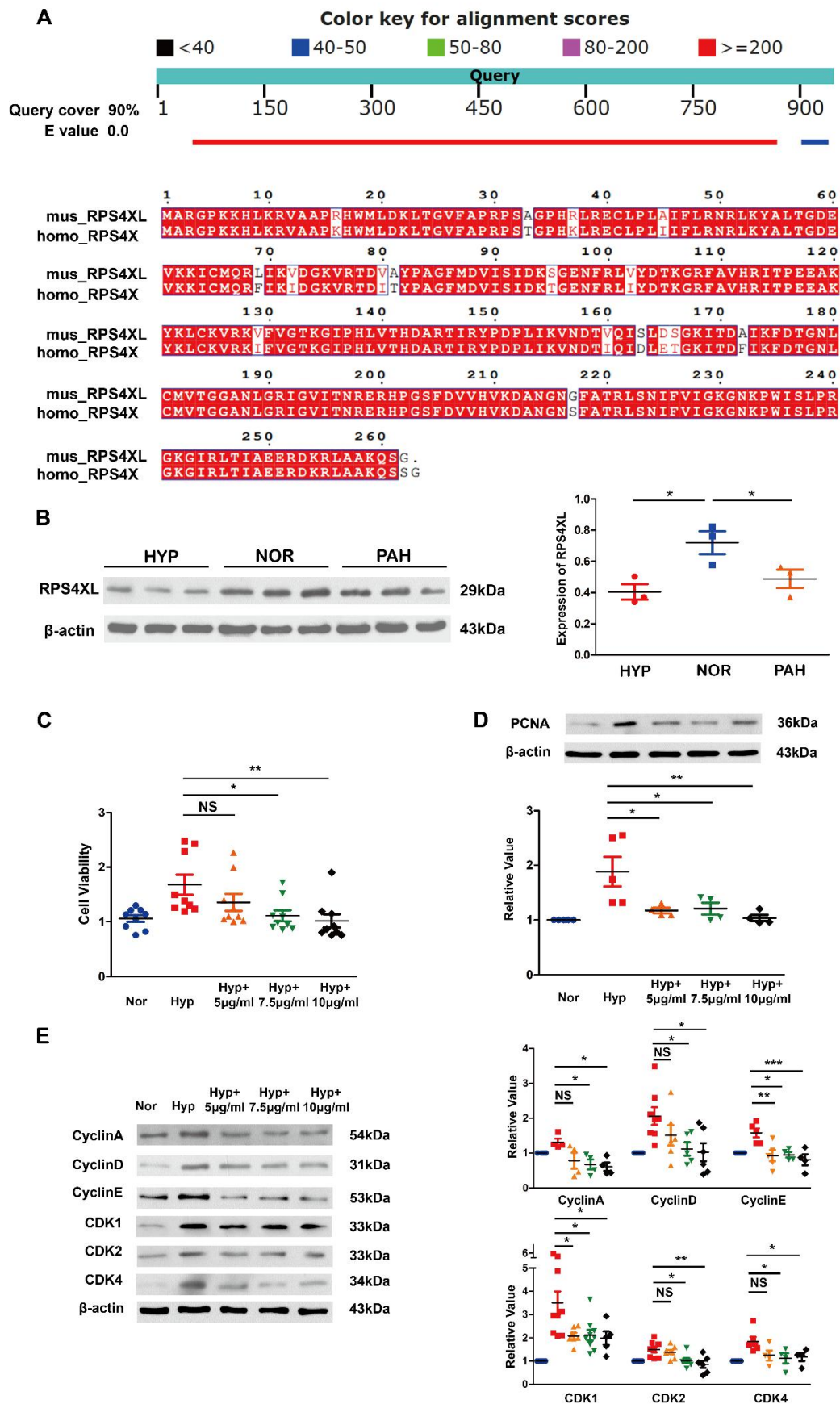
Figure S8



Supplemental figure 8. Rps4l-encoded peptide RPS4XL attenuates PASC

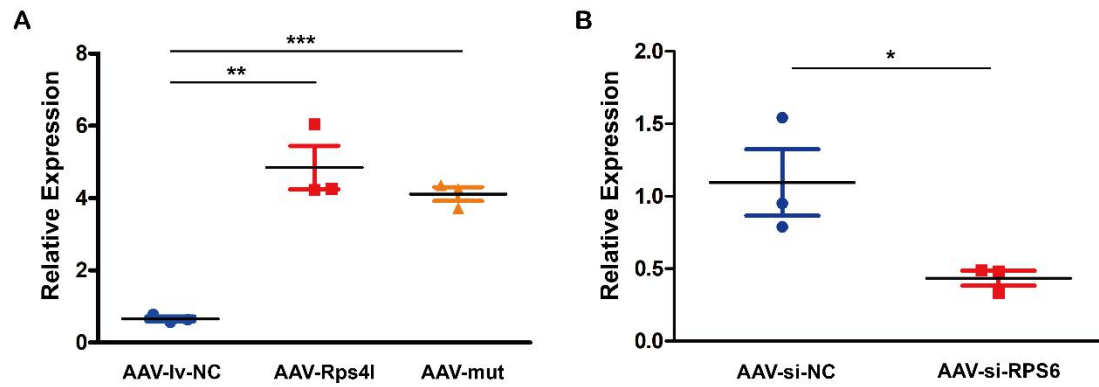
proliferation by inhibiting RPS6 phosphorylation. (A) MTT assay in hypoxic and control PASCs co-transfected with lvRps4l, ORFmut, or lv-NC and si-RPS6 or si-NC. (B) WB analysis of PCNA in hypoxic and control PASCs co-transfected with lvRps4l, ORFmut, or lv-NC and si-RPS6 or si-NC. (C) WB analysis of cyclin A, cyclin D, cyclin E, CDK1, CDK2, and CDK4 in hypoxic and control PASCs co-transfected with si-RPS6 or si-NC. (D) MTT assay in hypoxic and control PASCs simultaneously add 10ug/ml exogenous peptide RPS4XL and si-NC or si-RPS6. (E) WB analysis of PCNA in hypoxic and control PASCs simultaneously add 10ug/ml exogenous peptide RPS4XL and si-NC or si-RPS6. (F) WB analysis of cyclin A, cyclin D, cyclin E, CDK1, CDK2, and CDK4 in hypoxic and control PASCs simultaneously add 10ug/ml exogenous peptide RPS4XL and si-NC or si-RPS6. All values are represented as the mean \pm SEM (*p < 0.05, **p < 0.01, ***p < 0.001 and NS, no significance; n \geq 3). Nor, normoxia; Hyp, hypoxia.

Figure S9



Supplemental figures 9. The peptide RPS4XL is conserved in humans and inhibits the proliferation of human pulmonary artery smooth muscle cells induced by hypoxia. (A) Bioinformatics alignment of the homologous sequences of Rps4l-encoded peptide RPS4XL in human and mouse. (B) WB analysis of RPS4XL in hypoxic, control human PSMCs and pulmonary hypertension patient PSMCs. (C) MTT assay in hypoxic and control human PSMCs treated with RPS4XL with concentrations of 5 ug/ml, 7.5ug/ml or 10 ug/ml. (D) WB analysis of PCNA. (E) WB analysis of cyclin A, cyclin D, cyclin E, CDK1, CDK2, and CDK4 in hypoxic and control human PSMCs treated with RPS4XL with concentrations of 5 ug/ml, 7.5ug/ml or 10 ug/ml. All values are represented as the mean \pm SEM (* p <0.05, ** p <0.01 and NS, no significance; $n \geq 3$). Nor, normoxia; Hyp, hypoxia.

Figure S10



Supplemental figure 10. The efficiency of AAV9 overexpresses Rps4l, mutates

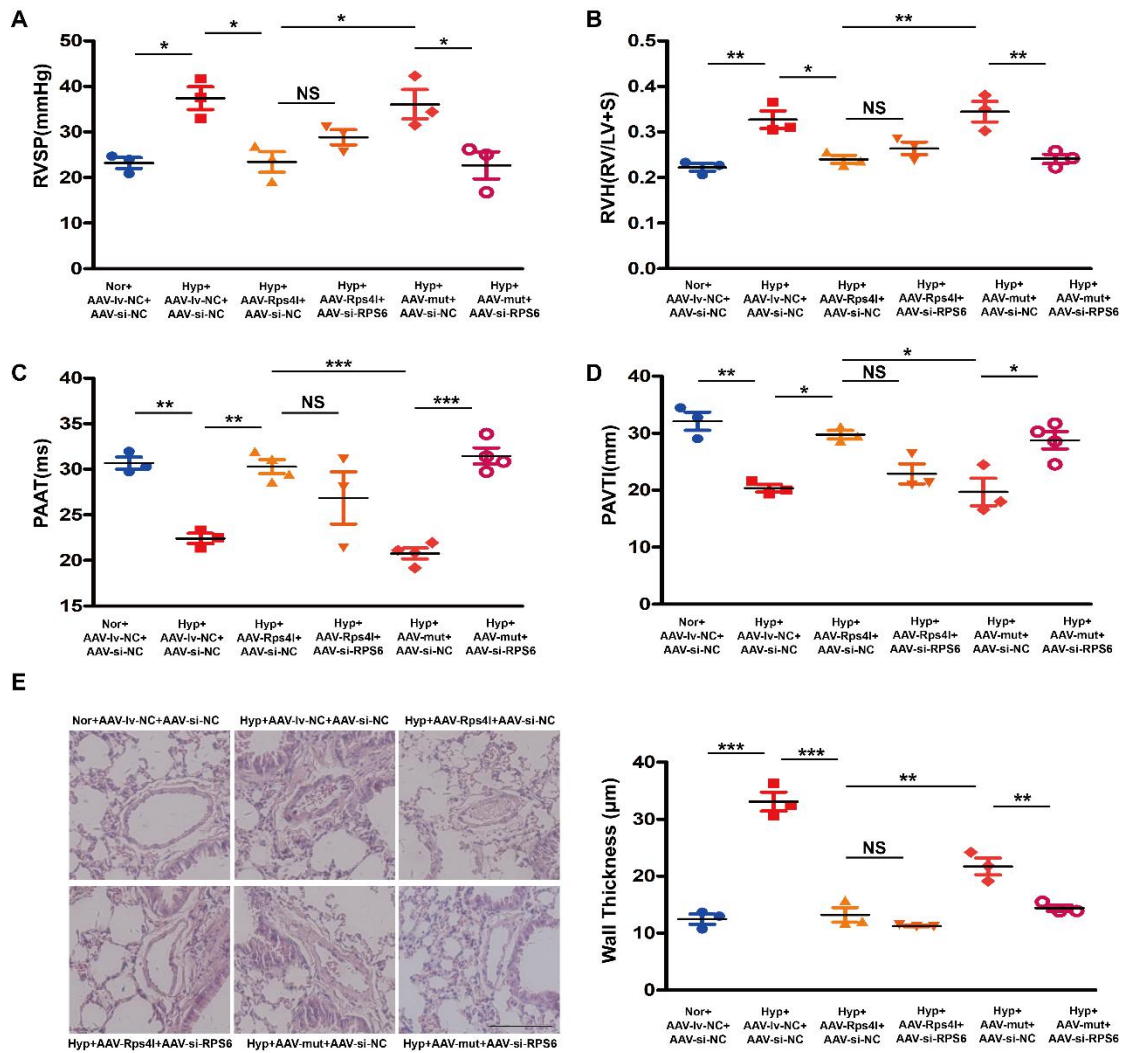
Rps4l and interferes with of RPS6. (A) qPCR for the efficiency of AAV9

overexpression of Rps4l and mut-Rps4l. (B) qPCR for the efficiency of AAV9

interference with RPS6. All values are represented as the mean \pm SEM (* $p < 0.05$,

** $p < 0.01$ and *** $p < 0.001$; $n \geq 3$).

Figure S11



Supplemental figure 11. RPS4XL blocks hypoxia-induced pulmonary hypertension in vivo through RPS6. (A-E) (A) RV systolic pressure (RVSP) (B) Right ventricular (RV)/left ventricular (LV)+S weight ratio (C) PAAT (D) PAVTI and (E) HE staining (Scale bar = 200 μ m) of hypoxic mouse model infected with AAV9-lv-NC, AAV9-lv-Rps4l, AAV9-lv-mut and AAV9-si-NC, AAV9-si-RPS6. All values are represented as the mean \pm SEM (* p < 0.05, ** p < 0.01, *** p < 0.001 NS, and no significance; $n \geq 3$). Nor, normoxia; Hyp, hypoxia.